

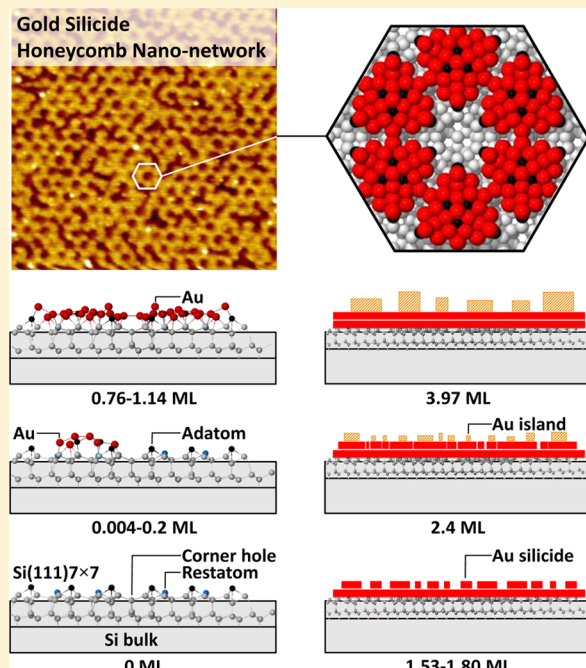
Two-Dimensional Self-Assembled Gold Silicide Honeycomb Nanonetwork on Si(111)7×7

Fatemeh R. Rahsepar, Lei Zhang, and K. T. Leung*

WATLab and Department of Chemistry, University of Waterloo, Waterloo, Ontario N2L 3G, Canada

Supporting Information

ABSTRACT: The growth evolution of Au on Si(111)7×7 at room temperature under ultrahigh vacuum conditions is studied by using scanning tunneling microscopy (STM) and X-ray photoelectron spectroscopy (XPS). Both STM filled-state and empty-state imaging show that on the 7×7 surface two distinct Au layers form one after another, each by connecting patches of adjoining Au clusters, before individual islands start to grow on top. XPS measurements of the same coverages reveal that Au exists as gold silicide in the two interfacial distinct layers and as metallic Au in the islands. The critical thickness of the gold silicide interface region is found to be two monolayers, which marks the transition from layer-by-layer to island growth. These results provide direct observation and chemical-state characterization of Au growth on Si(111)7×7 in the Stranski–Krastanov mode. Of special interest is the formation of the gold silicide honeycomb nanonetwork at 0.76 monolayer coverage, which is made up of six triangular Au clusters (around each corner hole) interconnected to one another at the dimer rows of the Si(111)7×7 substrate. With the corner holes of the 7×7 surface exposed, this new gold silicide nanonetwork, in effect, forms a two-dimensional template of nanopores (~1 nm in pore size) for molecular trapping application. The gold silicide honeycomb nanonetwork also offers a new conducting phase of fundamental interest to semiconductor device fabrication and to potential applications in biofunctionalization.



INTRODUCTION

As a noble metal, Au is well-known for its stability and inertness even at high temperature. However, Au has been found to readily react with Si, with the first report of an intermixed Au/Si interface dated back to four decades ago.¹ This unusual reactivity of Au toward Si is of fundamental interest. Furthermore, the catalytic property of Au in the nanoscale has also attracted a lot of attention because of its many potential technological applications. A large variety of preparation techniques have therefore been employed to grow Au on a Si surface, from single Au adatoms to clusters to nanoparticles to thick films. Growing Au on a clean, single-crystalline Si surface in ultrahigh vacuum is considered to be the best way to study the Au–Si reaction and the extent of this interaction, because complications due to oxide formation and grain boundaries could be minimized. Previous ultrahigh vacuum studies have focused exclusively on either the very early stage of formation of Au/Si interface² or a large Au coverage on Si.³ Single Au adatoms,⁴ dimers,⁵ and clusters with a proposed Au_6Si_3 structure⁶ have been observed on Si(111)7×7 at room⁷ and lower temperatures by using

scanning tunneling microscopy (STM). On the other hand, at a high Au coverage three-dimensional Au^{8,9} or gold silicide islands have been found by using photoemission^{10–12} and medium energy ion scattering.¹³ Along with the formation and location of the gold silicide in the growth stage, the growth mode of Au on Si is also of great interest in the literature. In general, the common growth mode of heteroepitaxial growth of metals on Si surfaces is the Stranski–Krastanov mode. In this so-called mixed growth mode, the initial two-dimensional layer-by-layer growth is switched to three-dimensional island growth at a certain critical thickness.¹⁴ While the growth mode of Au on Si(111) (with various postannealing temperatures) has been generally accepted to follow the Stranski–Krastanov mode,⁹ details about the growth evolution particularly near the critical thickness region remain unclear. In spite of the earlier efforts and this seemingly simple metal–semiconductor “benchmark” system, a consistent picture about the formation and location of

Received: February 6, 2014

Revised: March 28, 2014

Published: April 1, 2014

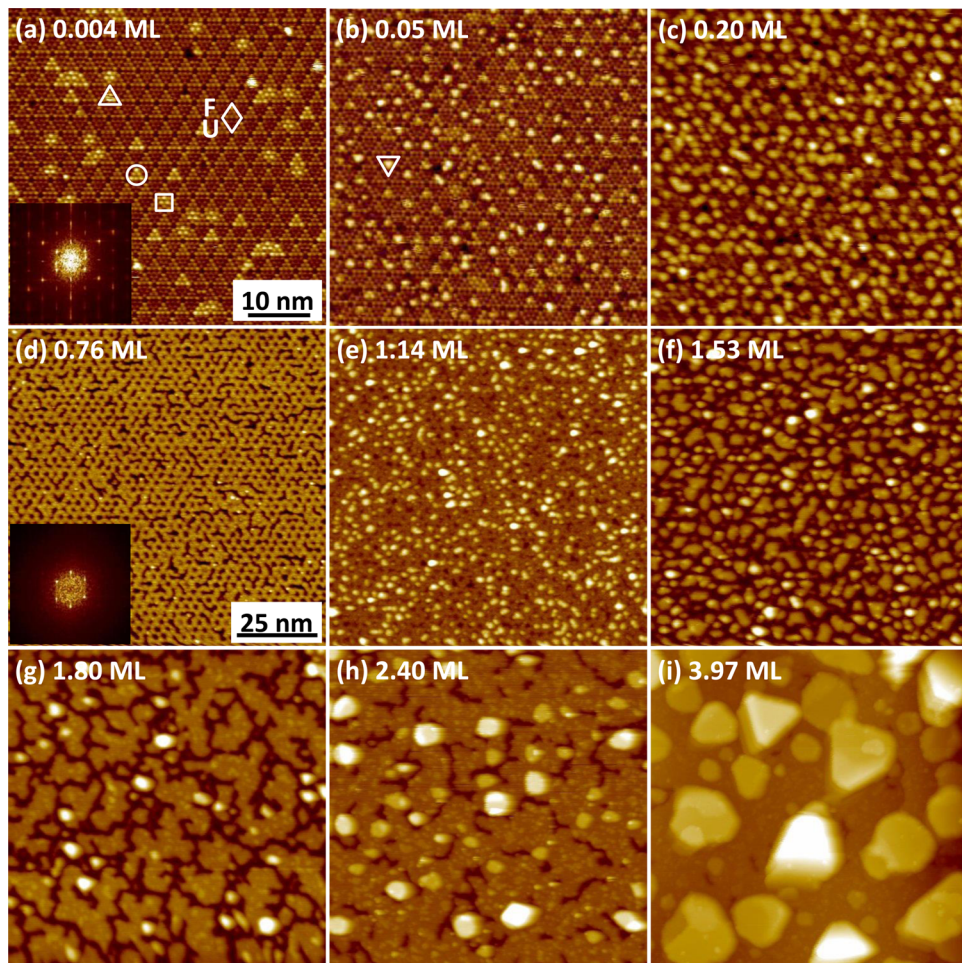


Figure 1. STM filled-state images of (a) 0.004, (b) 0.05, (c) 0.20, (d) 0.76, (e) 1.14, (f) 1.53, (g) 1.80, (h) 2.40, and (i) 3.97 ML of Au on Si(111)7×7 at room temperature, all collected with a sample bias of −2.0 V and a tunneling current of 0.2 nA. The fields of view for a–c and d–i are $50 \times 50 \text{ nm}^2$ and $100 \times 100 \text{ nm}^2$, respectively. The faulted and unfaulted half unit cells are marked by F and U, respectively, in panel a. Insets in panels a and d show the Fourier transforms of the respective images, in which the 1/7th fractional spots corresponding to the periodic (7×7) reconstruction are clearly evident.

gold silicide in the growth stage of Au on Si has not been reached.^{10–13,15,16} This important information is of fundamental interest to silicon device fabrication, particularly in areas of metal passivation. For example, the topmost layers of Au film on Si have been reported to be gold silicide,^{3,13,17} metallic Au,^{10,18} or Si-rich alloy.^{19,20} In the case of Au growth on Si(111)7×7 at room temperature, by using a combination of photoemission and ion scattering techniques, Hoshino et al. have reported the growth of two atomic layers (at an Au coverage of 5.2 monolayers) in the form of Au_3Si_2 on top of a metallic Au layer.¹³ Even more surprising was their observation that an increase in the Au dosage only led to an increase in the metallic Au layer thickness, with the top Au_3Si_2 layers remaining unchanged.¹³ In contrast, according to Kim et al.,¹⁰ a complete monolayer of metallic Au was formed on the top of a gold silicide interfacial layer. They drew this conclusion from their results obtained by positron-annihilation-induced Auger electron spectroscopy that was sensitive to just the topmost layer, together with conventional Auger electron spectroscopy.

Here, we study the growth evolution of Au on Si(111)7×7 at room temperature under ultrahigh vacuum conditions by correlating our STM images with our XPS spectra for the same coverage over a wide coverage range, from single adatoms to clusters to honeycomb nanonetwork and to islands. In

particular, the morphology of Au (i.e., wetting layers vs islands) can be directly inferred from the STM images, while the chemical states of Au with well-defined chemical shifts (i.e., gold silicide vs metallic Au) can be obtained from the XPS spectra. Together, these results can be used to resolve the existing controversies about the formation and location of gold silicide in the growth stage near the critical thickness region.

■ EXPERIMENTAL DETAILS

The experiments were performed in a five-chamber ultrahigh vacuum system (with a base pressure better than 5×10^{-11} mbar), which was equipped with an X-ray photoelectron spectrometer and a variable-temperature scanning tunneling microscope (Omicron Nanotechnology, Inc.).²¹ The 7×7 reconstruction of an n-type Si(111) sample ($2 \times 11 \text{ mm}^2$, 0.3 mm thick, and $0.005 \Omega \text{ cm}$ resistivity) was obtained by passing a direct current to flash-anneal the sample to $\sim 1200^\circ\text{C}$ for 10 s, followed by slow cooling to room temperature. This procedure produced large terraces of 7×7 reconstruction, as observed with STM. The clean 7×7 substrate was then transferred into a molecular beam epitaxy growth chamber, in which Au (99.999% purity) was deposited by thermal evaporation at 1040°C with the 7×7 substrate held at room temperature. Different doses of Au were exposed onto the 7×7

surface, and each exposure was performed onto a freshly cleaned 7×7 surface as described above. After each exposure, both STM and XPS measurements were performed on the same sample in the analysis chamber. STM experiments were conducted with a constant tunneling current mode using an atomically sharp W tip obtained by electrochemical etching. For XPS, Si 2p and Au 4f spectra were recorded with an overall energy resolution of 0.7 eV fwhm (for the Ag 3d_{5/2} photoline at 368.3 eV) using monochromatized Al K α X-ray (1486.7 eV) and an analyzer pass energy of 20 eV. The Au coverage was given in monolayers (ML), for which 1 ML corresponds to 7.83×10^{14} atoms/cm² assuming the Si atomic density of an unreconstructed Si(111) surface. The calibration of Au coverage was carried out using the following procedure: (1) count the numbers of Au adatoms in the STM images where only single Au adatoms and dimers exist (i.e., those obtained at very low Au coverages, e.g., Figure 1a); (2) measure the corresponding Au 4f XPS spectrum of the same sample; (3) establish a relation between the Au surface number density (using the Si atomic density of an unreconstructed Si(111) surface) and the Au 4f peak area; and (4) use this relation to calculate the Au coverages for other samples using their respective Au 4f peak areas. This procedure allowed us to correlate the chemical state information obtained from XPS for a specific coverage with the corresponding morphology information provided by STM.

RESULTS AND DISCUSSION

Figure 1 presents the STM filled-state images for various Au coverages from 0.004 to 3.97 ML on Si(111) 7×7 at room temperature. At the lowest Au coverage (0.004 ML, with a magnified image shown in Supporting Information, Figure S1), there are three notable features: sextets, triads, and scribbles. Briefly, the sextets (Figure 1a, circle) and the triads (Figure 1a, square), located respectively on the faulted (marked by F in Figure 1a) and unfaulted (marked by U in Figure 1a) half unit cells (HUCs), correspond to a single Au adatom rapidly moving among the six Si adatom sites within the respective HUCs.²² Closer examination of the sextet features shows that the corner-adatom protrusions appear brighter than the center-adatom protrusions, indicating a higher local density of states at the corner-adatom sites than the center-adatom sites. Similarly, in the unfaulted HUC the center-adatom protrusions forming the triad are brighter than the corner-adatom protrusions, as a result of a higher Au density of states at the center-adatom sites.⁴ The scribble feature (Figure 1a, up triangle) results from a fast moving Au dimer within a HUC.⁵ An increase in the Au coverage to 0.05 ML leads to formation of new triangular clusters with 3-fold symmetry (Figure 1b, down triangle) located at the centers of the HUCs. We hypothesize that these triangle features correspond to Au_xSi_y clusters, including, e.g., Au₉Si₃ in accord with our large-scale calculations based on the density functional theory (DFT) (Supporting Information). At 0.20 ML (Figure 1c), larger clusters appear within the HUCs. The corresponding empty-state image (Supporting Information, Figure S2) shows that these larger distorted triangle features have not covered the Si dimer walls. It should be noted that at this low coverage the 7×7 reconstruction remains clearly visible, with the dimer rows and corner holes unambiguously defining the registry of the original 7×7 surface.

Further increase in the Au coverage leads to larger clusters that completely fill the HUCs, some of which start to connect with clusters in neighboring HUCs. At 0.76 ML, the continued

increase in size of these clusters and the merging of adjacent clusters eventually produce a complete Au layer with a honeycomb pattern that fills the entire Si(111) 7×7 surface template with just the empty corner holes exposed. As demonstrated by the persistence of the 7×7 and related spots in the fast Fourier transform of the STM image (cf. insets of Figures 1d and 1a), this two-dimensional honeycomb nanonetwork evidently follows the registry of the underlying 7×7 unit cell template. Indeed, the sharp spots in the fast Fourier transform of the honeycomb nanonetwork indicate its remarkably high degree of ordering. Si atoms in the third layer (i.e., the layer containing the corner hole) remain intact, preserving the otherwise disrupted 7×7 unit cell. Further Au exposure leads to growth of the second layer on the honeycomb nanonetwork (Figure 1e), at which Au atoms accumulate either on top of the existing Au clusters in the first layer or above the empty corner holes, as more and more Au atoms escape the confines of the underlying 7×7 HUCs. At higher coverage, the Au atoms continue to grow into patches of similar height, without any registry to the 7×7 unit cell. At 1.53 ML, patch growth continues and these Au patches evidently become larger and cover up any trace of the first-layer honeycomb clusters and corner holes (Figure 1f). Since Au still exists as gold silicide at this coverage (discussed below), this suggests that the Si atoms in the third layer (i.e., the corner hole layer) of the reconstruction are involved in the reaction of Au and Si atoms, with Au atoms covering displaced Si center adatoms (Supporting Information, Figure S3). With further increase in the coverage to 1.80 ML (Figure 1g), the patches in the second Au layer join with one another and nearly cover the entire first Au layer. These STM images therefore show that the first two Au layers appear continuous and display a wetting property on the 7×7 surface.

As the coverage increases to 2.40 ML (Figure 1h), individual three-dimensional islands as large as ~ 7.0 nm start to grow on the second layer. The replacement of layer-by-layer growth to island growth indicates a Stranski-Krastanov growth mechanism. The critical layer thickness, often used to mark the transition from layer-by-layer to island growth mode, depends on the strain and chemical potential of the deposited film. For the present Au/Si(111) 7×7 case, the critical layer thickness is found to be two physical layers equivalent to ~ 2 ML of Au coverage, which is in excellent agreement with our XPS results (discussed below) and with the Auger electron spectroscopy data reported by Kim et al.¹⁰ With further increase in the coverage to 3.97 ML (Figure 1i), the metallic Au islands eventually exhibit regular triangular and polygon shapes, which indicates that these Au islands are single-crystalline and they prefer to grow along a specific direction (e.g., [111]).

To complement the above STM results on surface morphology during growth with the chemical-state information, we conduct XPS studies and show in Figure 2a the corresponding Au 4f spectra for the respective Au coverages shown in Figure 1. Evidently, the spectra are dominated by a prominent Au 4f_{7/2} (4f_{5/2}) peak near 84.6 eV (88.3 eV) over the entire coverage range. Above 2.90 ML, a second Au 4f_{7/2} (4f_{5/2}) feature emerges at 83.8 eV (87.4 eV) and appears to strengthen with increasing coverage. The primary and secondary features at their respective higher and lower binding energies are attributed to the gold silicide (Au_xSi for short) and metallic Au, respectively. This is in excellent accord with our earlier work on Au nanoparticles on Si(100),²³ which shows that the binding energy of Au 4f_{7/2} for gold silicide is 0.9 eV

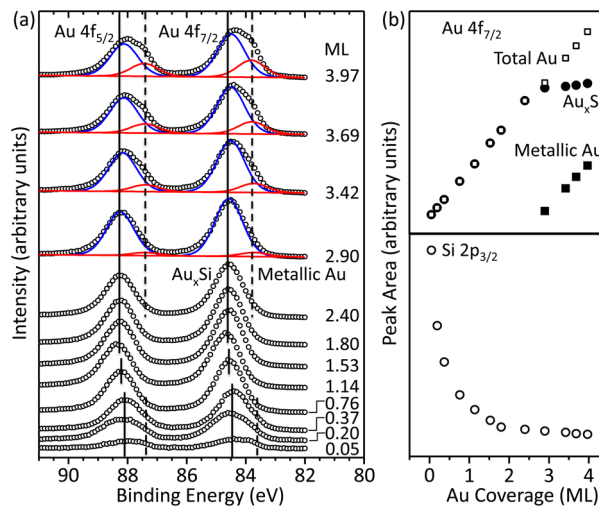


Figure 2. (a) XPS spectra of the Au 4f region for different Au coverages on Si(111)7×7 at room temperature. Solid and dashed lines mark the Au 4f peak positions for the gold silicide (Au_xSi) and metallic Au components, respectively. (b) Corresponding peak areas of the Au 4f_{7/2} peaks for Au_xSi and metallic Au components (along with their sum, marked as total), and of the Si 2p_{3/2} state at 99.3 eV.

higher than that for metallic Au. Au therefore adsorbs on Si first in the form of Au_xSi at the interface and then in the form of metallic Au with increasing coverage. It should be noted that, in the early growth stage (0.05, 0.20, 0.37 ML), there appears a discernible Au 4f_{7/2} (4f_{5/2}) feature near 83.6 eV (87.4 eV). At 0.05 ML coverage and as illustrated in the corresponding STM image (Figure 1b), Au is found to adsorb as highly mobile single adatoms and dimers. The high mobility of these Au adatoms indicates weak electronic interactions between Au atoms and the Si adatoms and that these “metal-like” Au atoms are loosely bound. It is also of interest to note that while the peak position of the metallic Au component is essentially stationary at 83.8 ± 0.1 eV for Au coverage above 2.4 ML, the metal-like Au feature found below 0.76 ML appears to be discernibly lower (83.6 eV). The minor shift in the Au_xSi component to lower binding energy could be due to the higher coordination of Au with Si before completing the first layer coverage and to less electron screening of the photon-excited core-level holes. The sharper Au 4f peaks of the Au_xSi component start at a coverage of 0.76 ML, which corresponds to the honeycomb nanonetwork shown in Figure 1d. At this Au coverage, the original Si(111)7×7 surface has, in effect, been transformed to a new two-dimensional honeycomb phase of Au_xSi component, which is not only structurally different (honeycomb vs 7×7) but also chemically different (Au_xSi vs Si). The relative intensities of Au 4f_{7/2} peaks for the Au_xSi and metallic Au 4f_{7/2} components (and their sum), along with that of the Si 2p_{3/2} peak, are plotted as functions of Au coverage in Figure 2b.

By combining the information provided by the STM images and XPS spectra, we obtain a more complete picture of Au growth on Si(111)7×7 near the critical thickness region. We summarize the growth evolution of Au on Si(111)7×7 in a schematic model shown in Figure 3. At very low coverage (0.004–0.05 ML), Au exists as highly mobile, metal-like Au adatoms and dimers shared among the Si adatom sites in the HUCs. As the coverage increases to 0.76 ML, these Au clusters increase in size and begin to merge with neighboring clusters, which consist of both metal-like Au and Au_xSi adspecies. At

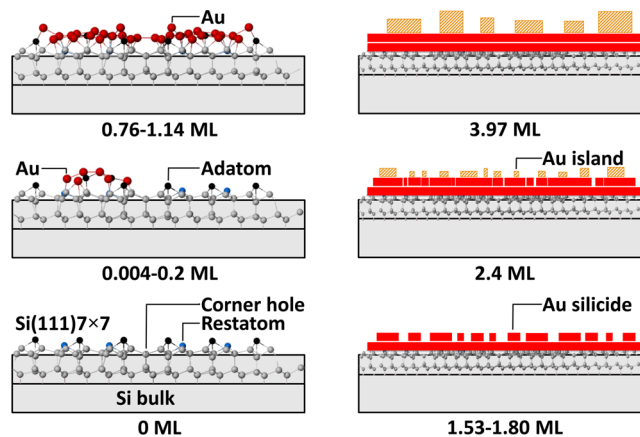


Figure 3. Schematic model of the growth evolution of Au on Si(111)7×7 at room temperature. Left column shows optimized structures based on DFT calculations for the early growth stage up to the formation of the first gold silicide layer. Right column shows the evolution to the second Au silicide layer and the formation of metallic Au islands.

0.76 ML, only the Au_xSi component is found, and these Au silicide adspecies form a remarkably well-ordered honeycomb two-dimensional phase, completely blanketing the Si(111)7×7 surface template. As most of the further deposited Au atoms are adsorbed on the first Au_xSi layer and they grow into the second layer, they remain as Au_xSi . Further increase in the coverage leads to eventual filling of the honeycombs to form a continuous first Au layer and to the growth of a second continuous Au_xSi layer. To understand the nature of the Au_xSi in the second layer, we perform large-scale DFT calculations, and the details of this computational work are given in the Supporting Information. For our calculations, we propose a Au_9Si_3 structure as a possible nucleation center for one of the six segments of the honeycomb unit, with each segment consisting of Au atoms located at three different Si sites (adatom, rest-atom, and pedestal atom sites) as illustrated in Supporting Information, Figure S3. The Au atoms in these segments essentially correspond to the majority of the first gold silicide layer, with some of center-adatom sites exposed. We believe that these unoccupied center-adatom sites are responsible for providing bonding to the Au atoms in the second Au_xSi layer. Above 2 ML coverage, the deposited Au atoms on top of the two continuous Au_xSi layers are sufficiently far from any Si atom, leaving them to react only with adjacent Au atoms, which leads to the formation of metallic Au islands. In agreement with the STM imaging is the coverage dependence of substrate Si 2p_{3/2} intensity shown in Figure 2b. In particular, the Si 2p_{3/2} intensity decreases exponentially from 0 to 2 ML Au coverage, consistent with the layer-by-layer growth mode. The Si 2p_{3/2} intensity then decreases at a much slower rate above 2 ML, indicative of the Au island growth. This also supports a critical thickness of 2 ML found for the Stranski–Krastanov growth. Our model is also consistent with the linear increase in the total Au 4f_{7/2} intensity with increasing Au coverage because the sampling depth of XPS is sufficiently large to cover the entire Au_xSi layers and the Au islands (Figure 2b).

CONCLUSION

We have studied the growth evolution of Au on Si(111)7×7 at room temperature under ultrahigh vacuum conditions by using

both STM and XPS. These combined results are crucial to provide support for the Stranski–Krastanov growth with the critical thickness of 2 ML that marks the formation of two Au_xSi layers followed by three-dimensional metallic Au island growth. It therefore seems unlikely that a metallic Au layer could form between the Au_xSi layers and the Si surface, as proposed by Hoshino et al. in their ion scattering study.¹³ In the layer-by-layer growth below 2 ML, Au atoms react with the top three Si layers of the 7×7 reconstruction (Si adatom layer, restatom layer, and layer containing the dimer rows and the corner holes) and form two continuous Au_xSi layers. Above 2 ML, Au atoms form large individual metallic Au islands. The intricate STM images reveal not only the Stranski–Krastanov growth mode, but also the formation of a Au_xSi honeycomb nanonetwork at 0.76 ML. Given the conducting property of Au_xSi , this honeycomb nanonetwork on Si(111)7×7 could provide an important passivation layer for device fabrication. Moreover, the Au_xSi honeycomb nanonetwork represents a unique nanoscale template of Au hexagonal grids (4 nm wide) and nanopores (~ 1 nm diameter). Upon functionalization by appropriate biomolecules such as cysteine or thiol-containing compounds, the Au_xSi honeycomb pattern also promises an important platform to build new applications for biosensing and molecular traps.

ASSOCIATED CONTENT

Supporting Information

Figures S1 and S2 (additional STM images), Figure S3 (DFT results), and description of DFT calculations. This material is available free of charge via the Internet at <http://pubs.acs.org>.

AUTHOR INFORMATION

Corresponding Author

*E-mail: tong@uwaterloo.ca. Tel: 519-888-4567 ext 35826.

Notes

The authors declare no competing financial interest.

ACKNOWLEDGMENTS

This work was supported by the Natural Sciences and Engineering Research Council of Canada.

REFERENCES

- (1) Narusawa, T.; Komiya, S.; Hiraki, A. Diffuse Interface in Si (substrate)–Au (evaporated Film) System. *Appl. Phys. Lett.* **1973**, *22*, 389–390.
- (2) Chizhov, I.; Geunseop, L.; Willis, R. F. Initial Stages of Au Adsorption on the Si(111)-(7×7) Surface Studied by Scanning Tunneling Microscopy. *Phys. Rev. B* **1997**, *56*, 12316–12320.
- (3) Braicovich, L.; Garner, C. M.; Skeath, P. R.; Su, C. Y.; Chye, P. W.; Lindau, I.; Spicer, W. E. Photoemission Studies of the Silicon-Gold Interface. *Phys. Rev. B* **1979**, *20*, 5131–5141.
- (4) Zhang, L.; Kim, Y.; Shim, H.; Lee, G. Adsorption of Au Atoms on Si(111)-(7×7) Studied by Using Scanning Tunneling Microscopy. *J. Korean Phys. Soc.* **2007**, *51*, 947–950.
- (5) Zhang, L.; Jeon, Y.; Shim, H.; Lee, G. Direct Observation of Hopping and Merging of Single Au Adatoms to Form Dimers on Si(111)-(7×7). *J. Vac. Sci. Technol. A* **2012**, *30*, 061406.
- (6) Wu, Y.; Zhou, Y.; Zhou, Ch.; Zhan, H.; Kang, J. Atomic Structure and Formation Mechanism of Identically Sized Au Clusters Grown on Si(111)-(7×7) Surface. *J. Chem. Phys.* **2010**, *133*, 124706.
- (7) Zhou, Y.; Wu, Q.-H.; Kang, J. STM Study of Au Adsorption on Si(111)-7×7 Surface: Voltage and Temperature Dependence. *J. Nanosci. Nanotechnol.* **2008**, *8*, 3030–3035.
- (8) Rota, A.; Martinez-Gil, A.; Agnus, G.; Moyen, E.; Maroutian, T.; Bartenlian, B.; Mégy, R.; Hanbücken, M.; Beauvillain, P. Au Island Growth on a Si(111) Vicinal Surface. *Surf. Sci.* **2006**, *600*, 1207–1212.
- (9) Kirakosian, A.; Lin, J.-L.; Petrovykh, D. Y.; Crain, J. N.; Himpel, F. J. Functionalization of Silicon Step Arrays I: Au Passivation of Stepped Si(111) Templates. *J. Appl. Phys.* **2001**, *90*, 3286–3290.
- (10) Kim, J. H.; Yang, G.; Yang, S.; Weiss, A. H. Study of the Growth and Stability of Ultra-Thin Films of Au Deposited on Si(100) and Si(111). *Surf. Sci.* **2001**, *475*, 37–46.
- (11) Yeh, J.-J.; Hwang, J.; Bertness, K.; Friedman, D. J.; Cao, R.; Lindau, I. Growth of the Room Temperature Au/Si(111)-(7×7) Interface. *Phys. Rev. Lett.* **1993**, *70*, 3768–3771.
- (12) Molodtsov, S. L.; Laubschat, C.; Shikin, A. M.; Adamchuk, V. K. Effects of Adatom Concentration on Au/Si(111) and Si/Au Interface Formation. *Surf. Sci.* **1992**, *269/270*, 988–994.
- (13) Hoshino, Y.; Kitsudo, Y.; Iwami, M.; Kido, Y. The Structure and Growth Process of Au/Si(111) Analyzed by High-Resolution Ion Scattering Coupled with Photoelectron Spectroscopy. *Surf. Sci.* **2008**, *602*, 2089–2095.
- (14) Baskaran, A.; Smereka, P. Mechanisms of Stranski-Krastanov Growth. *J. Appl. Phys.* **2012**, *111*, 044321.
- (15) Iwami, M.; Terada, T.; Tochihara, H.; Kubota, M.; Murata, Y. Alloyed Interface Formation in the Au-Si(111)2×1 System Studied by Photoemission Spectroscopy. *Surf. Sci.* **1988**, *194*, 115–125.
- (16) Landree, E.; Grozea, D.; Collazo-Davila, C.; Marks, L. D. UHV High-Resolution Electron Microscopy and Chemical Analysis of Room-Temperature Au Deposition on Si(001)-2×1. *Phys. Rev. B* **1997**, *55*, 7910–7916.
- (17) Abbati, I.; Braicovich, L.; Franciosi, A.; Lindau, I.; Skeath, P. R.; Su, C. Y.; Spicer, W. E. Photoemission Investigation of the Temperature Effect on Si–Au Interfaces. *J. Vac. Sci. Technol. B* **1980**, *17*, 930–935.
- (18) Narusawa, T.; Kinoshita, K.; Gibson, W. M.; Hiraki, A. Structure Study of Au–Si Interface by MeV Ion Scattering. *J. Vac. Sci. Technol. B* **1981**, *18*, 872–875.
- (19) Brillson, L. J.; Katnani, A. D.; Kelly, M.; Margaritondo, G. Photoemission Studies of Atomic Redistribution at Gold–silicon and Aluminum–silicon Interfaces. *J. Vac. Sci. Technol. A* **1984**, *2*, 551–555.
- (20) Cros, A.; Salvan, F.; Commandre, M.; Derrien, J. Enhancement of the Room Temperature Oxidation of Silicon by Very Thin Predeposited Gold Layers. *Surf. Sci. Lett.* **1981**, *103*, L109–L114.
- (21) Chatterjee, A.; Zhang, L.; Leung, K. T. Bidentate Surface Structures of Glycylglycine on Si(111)7×7 by High-Resolution Scanning Tunneling Microscopy: Site-Specific Adsorption via N-H and O-H or Double N-H Dissociation. *Langmuir* **2012**, *28*, 12502–12508.
- (22) Zhang, C.; Chen, G.; Wang, K.; Yang, H.; Su, T.; Chan, C. T.; Loy, M. M. T.; Xiao, X. Experimental and Theoretical Investigation of Single Cu, Ag, and Au Atoms Adsorbed on Si(111)-(7×7). *Phys. Rev. Lett.* **2005**, *94*, 176104.
- (23) Zhao, L.; Siu, A. C.-L.; Petrus, J. A.; He, Z.; Leung, K. T. Interfacial Bonding of Gold Nanoparticles on a H-Terminated Si(100) Substrate Obtained by Electro- and Electroless Deposition. *J. Am. Chem. Soc.* **2007**, *129*, 5730–5734.